

Astrochemistry of dense protostellar and protoplanetary environments

Ewine F. van Dishoeck

Abstract Dense molecular clouds contain a remarkably rich chemistry, as revealed by combined submillimeter and infrared observations. Simple and complex (organic) gases, polycyclic aromatic hydrocarbons, ices and silicates have been unambiguously detected in both low- and high-mass star forming regions. During star- and planet formation, these molecules undergo large abundance changes, with most of the heavy species frozen out as icy mantles on grains in the cold pre-stellar phase. As the protostars heat up their immediate surroundings, the warming and evaporation of the ices triggers the formation of more complex molecules, perhaps even of pre-biotic origin. Water, a key ingredient in the chemistry of life, is boosted in abundance in hot gas. Some of these molecules enter the protoplanetary disk where they are exposed to UV radiation or X-rays and modified further. The enhanced resolution and sensitivity of ALMA, Herschel, SOFIA, JWST and ELTs across the full range of wavelengths from cm to μm will be essential to trace this lifecycle of gas and dust from clouds to planets. The continued need for basic molecular data on gaseous and solid-state material coupled with powerful radiative transfer tools is emphasized to reap the full scientific benefits from these new facilities.

1 Introduction and overview

The study of exo-planetary systems and their formation is one of the fastest growing topics in astronomy, with far-reaching implications for our place in the universe. Intimately related to this topic is the study of the chemical composition of the gaseous and solid state material out of which new planets form and how it is modified in the dense protostellar and protoplanetary environments. Interstellar clouds are known

E.F. van Dishoeck

Leiden Observatory, Leiden University, P.O. Box 9513, 2300 RA Leiden, The Netherlands and Max-Planck Institute für Extraterrestrische Physik, Garching, Germany; e-mail: ewine@strw.leidenuniv.nl

to have a rich chemical composition, with more than 130 different species identified in the gas, ranging from the simplest diatomic molecules such as CO to long carbon chains such as HC₉N and complex organic molecules like CH₃OCH₃. Polycyclic aromatic hydrocarbons (PAHs) are a ubiquitous component of star-forming regions throughout the universe, and ices have been found to be a major reservoir of heavy elements in the coldest and densest clouds. Indeed, the gas, ice and dust undergo a rich variety of chemical transformations in response to the large changes in physical conditions during star- and planet formation, where temperatures vary from <10 K to more than 1000 K and densities from $\sim 10^4$ to $> 10^{10}$ H₂ molecules cm⁻³. Intense ultraviolet (UV) radiation and X-rays from the young star impact the envelopes and disks causing further chemical changes. At the same time, these chemical changes can also be used as diagnostics of the physical processes. Tracing this chemical and physical evolution in its diversity requires a combination of observations from infrared (IR) to millimeter (mm) wavelengths, where gaseous and solid material have their principal spectroscopic features and where the extinction is small enough to penetrate the dusty regions.

The different evolutionary stages in star- and planet formation are traditionally linked to their Spectral Energy Distributions (SEDs) (Lada 1999), which illustrate how the bulk of the luminosity shifts from far- to near-infrared wavelengths as matter moves from envelope to disk to star. In the standard scenario for the formation of an isolated low-mass star, the earliest stage is represented by a cold pre-stellar core which contracts as magnetic and turbulent support are lost. This phase is characterized by heavy freeze out of molecules onto the grains to form ices. Subsequent inside-out collapse forms a protostellar object which derives most of its luminosity from accretion and heats its immediate surroundings, resulting in evaporation of ices back into the gas phase and in an active high-temperature chemistry. Because the initial core has some angular momentum, much of the infalling material ends up in a dense rotating disk from which further accretion onto the star occurs. Soon after formation, a stellar wind breaks out along the rotational axis of the system and drives a bipolar outflow entraining surrounding cloud material. The main chemical characteristics of outflows are high temperature shock chemistry and sputtering of grains returning heavy elements to the gas. Low-mass young stellar objects (YSOs) in this embedded phase of star formation are often denoted as Class 0 and I objects.

Once the protostellar envelope has been dispersed, an optically visible pre-main sequence star with a disk is revealed, a so-called Class II object. Inside this disk, grains collide and stick owing to the high densities, leading to pebbles, rocks and eventually planetesimals which settle to the midplane and interact to form planets. High densities lead to freeze-out in the cold mid-plane, but UV radiation heats the surface layers leading to an active gas-phase chemistry. Changes in the mineralogical structure of the dust indicate thermal processing in the hot inner disk. Ices survive in the outer parts of the disk, providing the volatiles for atmospheres, oceans and possibly life on rocky planets. The remaining gas and dust which do not make it into planets or smaller (icy) bodies are gradually lost from the disk through a combination of processes, including photoevaporation and stellar winds.

The above scenario holds largely for low- and intermediate mass stars, with luminosities up to $\sim 10^3 L_{\odot}$. The formation of massive O and B stars is much more poorly understood due to larger distances, shorter timescales and heavy extinction. Recent observations show that the embedded phase of massive star formation can be divided into several stages. Massive pre-stellar cores with local temperature minima and density maxima represent the initial conditions. The next phase are the high-mass protostellar objects (HMPO) which contain a central young star surrounded by a massive envelope with a centrally peaked temperature and density distribution. HMPOs show signs of active star formation through outflows and/or masers. The next, related phase are the hot molecular cores which have large compact masses of warm and dense dust and gas, and high abundances of complex organic molecules. Finally, hyper-compact HII regions with pockets of ionized gas develop, but they have rather weak free-free emission since they are still confined to the star. The embedded phase ends when the ionized gas expands hydrodynamically and disrupts the parental molecular cloud, producing a classical compact HII region.

In this chapter, an overview will be given of the different chemical characteristics and their modifications during the various phases of star- and planet formation, both low- and high mass. Also, the use of molecules as probes of physical structure (temperature, density, radiation field, ionization fraction, geometry, ...) is discussed. Finally, the importance of chemistry and spectroscopic features in tracing evolutionary processes (timescales, grain growth, mixing, gap formation, ...) is emphasized. Note that our current knowledge is almost entirely based on spatially unresolved observations which encompass the entire star + disk + envelope system in a single beam. A key aspect of new facilities like ALMA, JWST, Herschel, SOFIA and future ELTs is that they will have the combined spatial and spectral resolution as well as the sensitivity to resolve the individual physical components and image the key chemical processes on all relevant scales. Other recent reviews on this topic include (van Dishoeck 2006; Ceccarelli et al. 2007; Bergin et al. 2007; Bergin & Tafalla 2007).

Astrochemistry is a highly interdisciplinary subject and many of the basic chemical processes that occur under the exotic conditions in space are not yet well understood. Continued interaction of astronomers with chemists and physicists to determine the basic atomic and molecular data is essential to make progress.

2 Infrared and submillimeter observations

The two main observational techniques for studying gaseous and solid-state material in protostellar regions are infrared and (sub)millimeter spectroscopy (Table 1). Both techniques have their strengths and weaknesses, and a combination of them is essential to obtain a full inventory and probe the different physical processes involved (Table 2).

Table 1 Need for broad wavelength coverage to study astrochemistry and star formation

Radiation	Mid-IR 3-28 μm	Far-IR 28-350 μm	Submm 0.3-7 mm	Radio ≥ 1 cm
Continuum	Warm dust	Cooler dust, SED peak	Cold dust	Large grains (pebbles), ionized gas
Broad features: solids	Silicates, ices, oxides, PAHs	(Hydrous) silicates, ices, carbonates, PAHs
Narrow lines: gas	Simple (symmetric) molecules	H ₂ O, OH, O I hot CO, C II	CO, myriad of simple + complex molecules, O ₂	Heavy complex mol. H I, masers

2.1 Infrared spectroscopy

At infrared wavelengths, the vibrational bands of both gas-phase and solid-state material can be detected, including those of symmetric molecules like CH₄ and C₂H₂. The most abundant molecule in the universe, H₂, also has its principle rotational transitions at mid-infrared wavelengths. Resolving powers $R = \lambda/\Delta\lambda$ range from a few $\times 10^2$ up to 10^5 , which is sufficient to resolve intrinsically broad solid-state features but not the narrower profiles of quiescent gas. In protostellar sources, bands of silicates, cold ices and gases are seen in *absorption* superposed on the infrared continuum due to hot dust close to the young star (Fig. 1). Thus, these observations probe only a pencil-beam line-of-sight and are more sensitive to the warm inner part than the submillimeter data. Toward pre-main sequence stars with disks, features of silicates, PAHs and hot gases are usually found in *emission*, originating in the warm surface layers and the hot inner disk. In near edge-on geometries, the bands occur in absorption. Because of the limited spectral resolution and sensitivity, abundances down to $10^{-7} - 10^{-8}$ with respect to H₂ can be probed, sufficient to detect the major O, C and N-bearing species but not the minor ones.

Only a small fraction of the infrared wavelength range can be observed from Earth. The *Infrared Space Observatory* (ISO, 1995–1998) provided the first opportunity to obtain complete 2.5–200 μm mid-infrared spectra above the Earth’s atmosphere at $R = 200 - 10^4$ but was limited in sensitivity to YSOs $10^3 - 10^5$ times more luminous than the Sun (for review, see van Dishoeck 2004). The *Spitzer Space Telescope*, launched in 2003, has orders of magnitude higher sensitivity and can obtain 5–40 μm spectra of YSOs down to the brown dwarf limit, albeit only at low resolution $R = 50 - 600$. The slits of both *ISO* and *Spitzer* are large, typically $> 10''$, so that most emission is spatially unresolved.

Complementary ground-based spectra can be obtained from 8–10m class telescopes in atmospheric windows at 3–20 μm . These facilities have two advantages: R up to 10^5 can be achieved and emission can be spatially resolved on subarcsec scales, comparable to those of disks (Table 2).

Table 2 Chemical characteristics of YSOs

Component	Size ^a ($''$)	Chemical characteristics	Submillimeter diagnostics	Infrared diagnostics
Pre-stellar cores	60	Low-T chemistry, Heavy freeze-out	Ions, deuterated, simple mol. (N_2H^+ , H_2D^+)	Simple ices (H_2O , CO_2 , CO)
Outer cold envelope	20	Low-T chemistry, Heavy freeze-out	Ions, deuterated, simple mol. (N_2H^+ , HCO^+ , $\text{H}_2\text{CO}\dots$)	Ices (H_2O , CO_2 , CO , $\text{CH}_3\text{OH}?$)
Inner warm envelope	1–2	Evaporation, X-rays (CO^+ , OH^+ , ...)	High T_{ex} (H_2CO , CH_3OH , CO , CO_2)	High gas/solid, High T_{ex} , Heated ices
Hot core	≤ 1	Evaporation, High-T chemistry	H_2O , Complex organics (CH_3OCH_3 , CH_3CN)	Hot gas (HCN , NH_3 , HNCO)
Outflow: direct impact	<1–20	Shock chemistry, Sputtering cores	H_2O , OH, Si- and S-species (SiO , SO_2)	H_2 , Atomic lines ([O I], [Si II], [S I])
Outflow: gentle impact	<1–20	Sputtering ices	Ice products (CH_3OH , H_2O , ..)	H_2
Outer disk: surface	~ 2	UV irradiation, Ion-molecule	Ions, radicals (CN/HCN , HCO^+)	PAHs, heated ices (NH_4^+)
Outer disk: midplane	~ 2	Heavy freeze-out,	Deuterated mol. (DCO^+ , H_2D^+)	...
Inner disk	≤ 0.02	Evaporation, High-T chemistry, X-rays	...	Silicates, PAHs, [Ne II], CO , H_2 , hot gas (H_2O , C_2H_2 , HCN)

^a Typical angular size for a low-mass YSO at 150 pc, or a high-mass YSO at 3 kpc.

2.2 Submillimeter spectroscopy

At (sub)millimeter wavelengths, the pure rotational lines of molecules are seen in emission. Only gaseous molecules with a permanent electric dipole moment can be observed, but not symmetric molecules like H_2 , N_2 , CH_4 , and C_2H_2 nor solid-state species. O_2 only has weak magnetic dipole transitions. The level spacing scales with $BJ(J+1)$, with J the rotational quantum number and B the rotational constant, which is inversely proportional to the reduced mass of the system. Thus, light hydrides such as H_2O , OH, CH, ... have their lowest transitions at submillimeter/far-infrared wavelengths, whereas those of heavy molecules like CO occur at longer wavelengths. A big advantage is that the heterodyne receivers naturally have very high resolution $R \geq 10^6$, so that the line profiles are fully resolved, providing information on dynamical processes occurring in the protostellar environment. Thus, infall, outflow and rotation can in principle be kinematically distinguished. Also, the sensitivity is very high: molecules with abundances as low as a few $\times 10^{-12}$ can be seen. Detection of linear molecules is favored compared with heavy asymmetric rotors because their population is spread over fewer energy levels.

Because the lines are in emission and can be readily excited by collisions even in cold gas, the spatial distribution of the molecule can be mapped. However, the angular resolution of the most advanced single-dish telescopes is only $\sim 15\text{--}20''$ which corresponds to a linear scale of a few thousand AU at the distances of the nearest

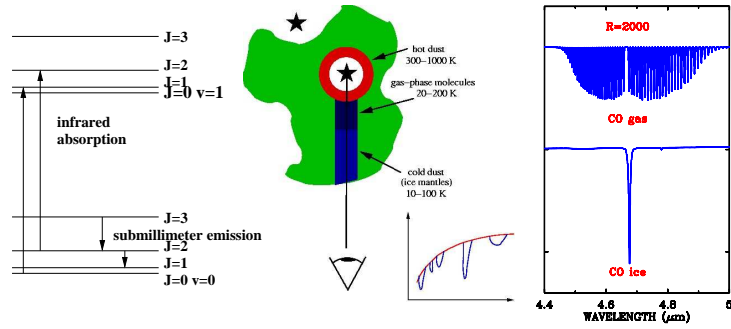


Fig. 1 Left: Energy level diagram showing typical (sub)millimeter and infrared lines. Middle: Cartoon illustrating infrared absorption line observations toward an embedded young stellar object. Right: Laboratory spectra of gas-phase and solid CO. Note that gas and ice can readily be distinguished at a resolving power $R = 2000$ and higher. The gas-phase CO spectrum gives direct information on the excitation temperature of the molecule since the individual lines originate from levels with different energies (see left panel).

star-forming regions of ~ 150 pc. Since typical sizes of protostellar envelopes are about 3000 AU, the single-dish beams encompass the entire protostellar envelope and are much larger than protoplanetary disks which have radii of order 100 AU. This means that the different chemical and physical regimes are ‘blurred’ together in a single spatial pixel, and that the data are generally more biased toward the cold, outer part.

Direct information on smaller spatial scales can be obtained by (sub)millimeter interferometry, which can reach resolutions down to $\sim 1''$ or ~ 50 AU. However, sensitivities of existing arrays are still limited and chemical surveys have not yet been feasible. Fortunately, the fact that molecules have so many different lines and transitions can be put to good use: single-dish observations of lines with a range of excitation conditions combined with detailed radiative transfer modeling can provide constraints on physical and chemical gradients on scales much smaller than the beam, down to a few $''$ (see below).

2.3 From intensities to physical conditions and abundances

The rotational and vibrational levels are excited by a combination of collisional and radiative processes. In the simplest case of a 2 level system, the critical density $n_{\text{cr}} = A_{ul}/q_{ul}$, where A_{ul} is the Einstein A constant for spontaneous emission and q_{ul} the rate coefficient for collisional de-excitation. Since A_{ul} is proportional to $\mu^2\nu^3$ with μ the dipole moment of the molecule, n_{cr} increases with frequency ν . Also, the rotational energy level separation of (linear) molecules is proportional to the quantum number J . Thus, the higher frequency, higher J transitions probe regions

with higher densities and temperatures. For example, the critical density of the CS $J=2-1$ transition at 97 GHz is $8 \times 10^4 \text{ cm}^{-3}$ ($E_u=7 \text{ K}$), whereas that of the $7-6$ transition at 346 GHz is $3 \times 10^6 \text{ cm}^{-3}$ ($E_u=66 \text{ K}$). For optically thick lines, line trapping will lower the critical densities. CO has a particularly small dipole moment, at least 20 times smaller than that of CS and other commonly observed species. Combined with its high abundance of $\sim 10^{-4}$ with respect to H_2 , this implies that CO is readily excited and detected in molecular clouds, even at densities as low as 10^3 cm^{-3} .

The translation of the observed intensities to chemical abundances, temperatures and densities requires a determination of the excitation of the molecule and an understanding of how the photon is produced in the cloud and how it makes its way from the cloud to the telescope. Significant progress has been made in recent years in the *quantitative* analysis of molecular line data through the development of rapid, accurate and well-tested radiative transfer codes which can be applied to multi-dimensional geometries (for overview, see van Zadelhoff et al. 2002).

2.4 Importance of laboratory astrophysics

The computation of the excitation of gas-phase molecules requires availability of accurate frequencies, radiative rates and collisional rate coefficients with the main collision partner, usually H_2 . For atoms, large data bases are available thanks to many decades of dedicated work by physicists in laboratories across the globe, allowing astronomers to readily interpret their optical and X-ray spectra. For molecules, such information is much more limited. In molecular clouds, the main collision partner is H_2 and state-to-state collisional rate coefficients are in principle required for both para- H_2 , $J=0$ (cold clouds) and ortho- H_2 , $J=1$ (warm regions). In practice, such data are available for only a few molecules and H_2 $J=0$ is usually taken as the main collision partner. Much of the molecular data gathered over the last 30 years from laboratory experiments and quantum-chemical calculations has been summarized by (Schöier et al. 2005) and made publicly available through the Web¹ together with a simple on-line radiative excitation code. New results, especially those coordinated through the EU ‘Molecular Universe’ network program², are being added. Nevertheless, accurate collision rates are still lacking for many astrochemically important molecules, especially the larger ones. The analysis of observational data on these species is often limited to the simple rotation diagram approach, in which it is assumed that the level populations can be characterized by a single excitation temperature and that the lines are optically thin (see §4.3 for example).

PAHs are a special class of very large molecules. Huge efforts have been made in the last decade to determine the basic spectroscopy and intensities of neutral and ionic PAHs by a variety of experimental and theoretical methods. (e.g., Hudgins &

¹ <http://www.strw.leidenuniv.nl/~moldata>

² <http://molecular-universe.obspm.fr/>

Allamandola 1999³; see review by Tielens 2008). One problem is that most studies are still limited to the smaller PAHs with up to about 30 carbon atoms, whereas the PAHs seen in interstellar and circumstellar regions are likely somewhat larger, containing up to 100 carbon atoms. Another problem is that many of the experiments have been done using matrix isolation techniques rather than in the gas phase, introducing shifts which are a priori unknown.

For solid-state species, information on infrared band positions, profiles and strengths are needed for analysis. Because these quantities depend on specific composition, e.g., whether the material is in pure or mixed form, large series of experiments are needed. For ices, systematic studies have been performed by a variety of groups (e.g., Hudgins et al. 1993; Gerakines et al. 1996; Öberg et al. 2007), with data available through the Web⁴. For silicates and oxides, the Jena database⁵ (e.g., Jaeger et al. 1998) is an invaluable resource for interpreting mid-infrared spectra.

Besides basic spectroscopy, there continues to be a great need for basic reaction rates of gas-phase processes from 10–1000 K (ion-molecule, neutral-neutral, radiative association, dissociative recombination), of reactions under the influence of UV radiation or X-rays (photodissociation, photoionization) and of reactions between the gas and the grains (e.g., H₂ formation on silicates; molecule formation on and in ices, binding energies). Summaries of rate coefficients are publicly available from UMIST⁶ and Ohio state⁷. Ultimately, the science return from the new billion dollar/Euro/Yen investments will be limited by our poor knowledge of these basic processes.

3 Cold clouds and pre-stellar cores

3.1 Dense starless clouds

Catalogs of isolated dark clouds and globules have been available for nearly a century. Some of them have become favorite targets of astrochemical studies, in particular the starless core TMC-1. Its conditions, $T \approx 10$ K and $n \approx 2 \times 10^4$ cm⁻³, are average of those of other cold dense clouds, but this core shows a remarkable variety of molecules. In particular, the unsaturated long carbon chains — e.g., HC₅N, HC₇N, HC₉N, C₄H, C₆H — have all been detected with relatively high abundances. An exciting recent discovery is that negative ions such as C₆H⁻ and C₈H⁻, which have long been neglected in astrochemical models, are present at abundances of 1–5% of their neutral counterparts (McCarthy et al. 2006; Brünken et al. 2007).

³ <http://www.astrochem.org/databases.htm>

⁴ <http://www.strw.leidenuniv.nl/~lab>

⁵ <http://www.astro.uni-jena.de/Laboratory/Database/databases.html>

⁶ <http://www.udfa.net>

⁷ <http://www.physics.ohiostate.edu/~eric/research.html>

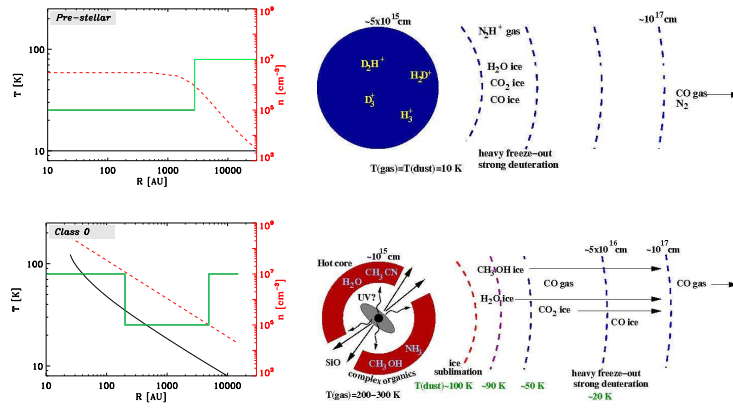


Fig. 2 Physical and chemical structure of a prestellar and a protostellar (Class 0) object. Left: density (red), temperature (black) and typical abundance (green) profiles. Right: cartoons illustrating the main chemical characteristics of each stage (based on Jørgensen et al. 2005, van Dishoeck & Blake 1998).

Clouds such as TMC-1 are traditionally used as benchmarks for pure gas-phase astrochemical models. Reasonable agreement with the observed abundances (within factors of 3) is obtained for the majority of species if TMC-1 is assumed to be ‘chemically young’, i.e., if the time since most of the carbon was in atomic form is only $\sim 10^5$ yr (e.g., Wakelam et al. 2006). This time most likely refers to the period elapsed since the dense cloud formed out of the more diffuse gas, but any other event that may have replenished atomic carbon in the cloud could also have reset the ‘clock’. However, the inclusion of gas-grain interactions and use of different elemental abundance ratios may affect these conclusions. Also, the recent discovery of the saturated propene molecule, CH_2CHCH_3 , which was not included or predicted in any models, casts doubt on their completeness (Marcelino et al. 2007). Indeed, the role of unobservable (at submm) molecules such as the bare carbon-chains C_2 and C_3 and saturated hydrocarbons like CH_4 and C_2H_6 is still poorly understood in dark clouds.

3.2 Pre-stellar cores

A subset of dark clouds with a clear central density concentration have been identified recently. These so-called pre-stellar cores are believed to be on the verge of collapse and thus represent the initial conditions for low-mass star formation (for review, see Bergin & Tafalla 2007). The physical and chemical state of these clouds is well established on scales of few thousand AU by single dish millimeter observations combined with extinction maps. The cores are cold, with temperatures varying

from 10–15 K at the edge to as low as 7–8 K at the center, and have density profiles that are well described by Bonnor-Ebert profiles. It is now widely accepted that most molecules are highly depleted in the inner dense parts of these cores (Caselli et al. 1999; Bergin et al. 2002): images of clouds such as B68 show only a ring of $C^{18}O$ emission, indicating that more than 90% of the CO is frozen out toward the center.

This ‘catastrophic’ freeze-out of CO and other molecules has also been probed directly through observations of ices as functions of position in the cloud. Owing to the increased sensitivity of ground-based 8-10m IR telescopes, *Spitzer* and *Akari*, it is now possible to make maps of ice abundances on the same spatial scale ($\sim 15''$) as those of gas-phase molecules, by taking spectra toward closely spaced background or embedded stars (Pontoppidan et al. 2004). The main features seen in mid-IR spectra are the 9.7 and 18 μm Si-O stretch and bending modes of the silicate grain cores, together with ice bands of relatively simple species (Fig. 3). H_2O ice, seen through its 3 and 6 μm bands, has the largest abundance, $\sim (0.5 - 1.5) \times 10^{-4}$ with respect to H_2 , whereas the combined contribution of CO and CO_2 may be as high as that of H_2O . Thus, the ices are a major reservoir of the heavy elements in cold clouds, exceeding even that of gaseous CO. Indeed, toward the center of the ρ Oph F core at least 60 % of CO is observed to be frozen out (Pontoppidan 2006).

Another chemical characteristic of cold cores is their extreme deuterium fractionation: doubly and even triply deuterated molecules like D_2CO , NHD_2 , ND_3 , and CD_3OH have been found with abundances that are enhanced by up to 13 orders of magnitude compared with the overall $[D]/[H]$ ratio (e.g., Lis et al. 2002; Parise et al. 2004). The origin of this strong deuteration is now understood to be directly linked to the observed heavy freeze-out: the basic ions H_3^+ and H_2D^+ , which initiate much of the low-temperature ion-molecule chemistry and deuteration, are enhanced significantly when their main destroyer, CO, is depleted onto grains. Grain surface chemistry may also play a role (Tielens 1983). Models predict that D_3^+ can become as abundant as H_3^+ (Roberts et al. 2003) and lines of both H_2D^+ and D_2H^+ have indeed been detected in cold clouds at submillimeter wavelengths (Caselli et al. 2003; Vastel et al. 2004). These ions may well be the best probes of the ionization fraction and kinematics in regions where all heavy molecules are depleted.

The freeze-out of CO is reflected in the abundances of many other molecules, either through correlations or anti-correlations (Jørgensen et al. 2004b). A striking example of the latter case is N_2H^+ , which, like H_3^+ and H_2D^+ , is mainly destroyed by reactions with CO. The binding energy of its precursor, N_2 , to ice is comparable to that of CO (Öberg et al. 2005), but the lack of a rapid gas-phase destruction channel together with the boost in H_3^+ keeps the N_2H^+ abundance high even if some N_2 is frozen out. Thus, N_2H^+ is an excellent and easy to observe tracer of the densest and coldest parts of cores.

The above discussion focussed on low-mass cores. Massive cold cores which likely represent the initial conditions for high mass star formation are only just starting to be identified, for example as infrared dark clouds. Their chemical character-

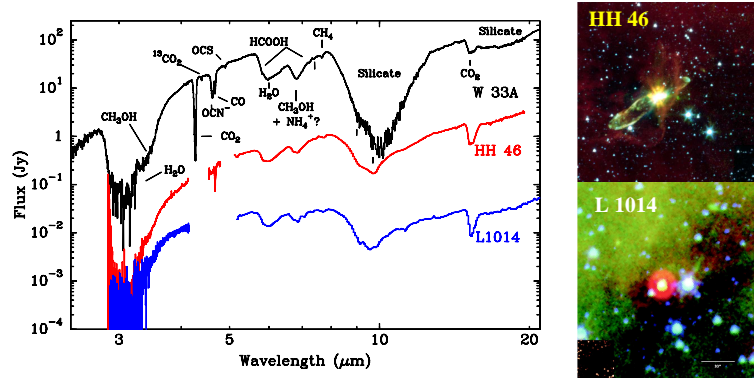


Fig. 3 Ices observed toward protostars with a large range of luminosities. Top: W 33A ($\sim 10^5 L_{\odot}$) from Gibb et al. (2000b); Middle: HH 46 ($\sim 10 L_{\odot}$) from Boogert et al. (2004); Bottom: L 1014 ($\sim 0.1 L_{\odot}$) from Boogert et al. (2008). Note the similarity in major ice features between high-mass and substellar mass YSOs. Right: Spitzer image of HH 46 IRS and its bipolar outflow (top; Noriega-Crespo et al. 2004) and of L 1014 (bottom; Young et al. 2004).

istics are likely to be similar to those of the low-mass pre-stellar clouds, in particular heavy freeze-out and strong deuteration toward the center (Pillai et al. 2007).

4 Embedded protostars

4.1 Cold outer envelope: ices

Ices are a prominent component of protostellar systems. With *Spitzer*, infrared spectra have now been observed toward several dozen low-mass YSOs including some of the most deeply embedded Class 0 YSOs and sources of substellar luminosity (Boogert et al. 2008) (Fig. 3). At first sight, all spectra look remarkably similar, not only to each other, but also to those toward much more luminous YSOs (HMPOs) and background stars. This implies that most ices are formed prior to star formation, and that orders of magnitude higher luminosities do not result in major changes in the ice composition. The detected species are consistent with a simple theory of grain surface chemistry put forward 25 years ago (Tielens & Hagen 1982), in which the major ice components are those formed by hydrogenation of the main atoms and molecules arriving from the gas on the grains. Thus, O, C, and N are hydrogenated to H_2O , CH_4 , NH_3 and CO is hydrogenated to H_2CO and CH_3OH , a reaction confirmed in the laboratory (Watanabe et al. 2004). The origin of CO_2 ice is

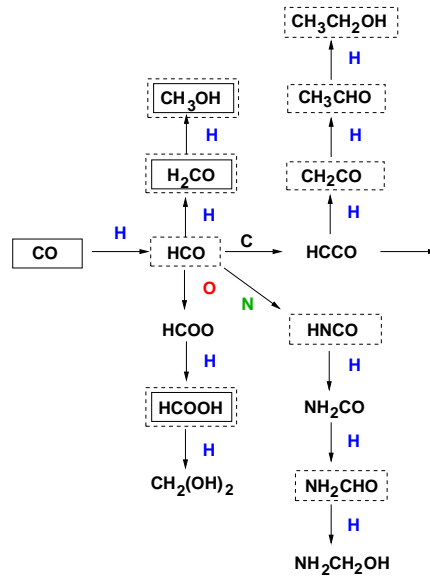


Fig. 4 Grain surface chemistry scheme leading to more complex organics proposed by Tielens & Charnley (1997). Solid rectangular boxes contain molecules which have been detected in interstellar ices, whereas dashed boxes indicate molecules that have been detected in the gas phase.

not yet fully clear, but likely involves reactions of CO with either O or OH. Reactions of CO with both H, O, C and N may lead to more complex organics (Fig. 4), although not all reactions in this scheme have yet been confirmed in the laboratory (Bisschop et al. 2007a).

On closer inspection, differences in ice composition are found, both between different types of sources and within one class of objects. In particular, abundances of minor species like CH₃OH, OCN⁻ and NH₃ vary by more than an order of magnitude among the low-mass YSOs and even on spatial scales as small as 1000 AU (Pontoppidan et al. 2004; van Broekhuizen et al. 2005). Since these molecules are the precursors of more complex organic species formed in the gas, one of the main future challenges is to understand the origin of these large abundance variations. Is this due to passive heating of the ices, or are UV radiation or cosmic ray bombardment (i.e., different forms of ‘energetic processing’) involved? The line profiles of solid CO, CO₂ and the carrier of the 6.8 μm feature (likely NH₄⁺, (Schutte & Khanna 2003)) show subtle changes which are related to heating of the ices up to at least 50 K (Keane et al. 2001; Boogert et al. 2008). At such temperatures, various atoms and radicals stored in the ices become mobile and lead to a rich chemistry (Garrod & Herbst 2006). An open question is to what extent complex organic molecules are formed on the grains during this heating phase rather than in the ‘hot core’ gas (see §4.3).

4.2 Warm inner envelopes: ice evaporation

Once the protostars have formed, they heat the envelopes from the inside, setting up a strong temperature gradient (see Fig. 2). As a result, molecules will evaporate from the grains back to the gas in a sequence according to their sublimation temperatures. The most volatile species like CO and N₂ will start to evaporate around 20 K in the outer envelope, whereas more strongly bound molecules like H₂O only evaporate around 100 K in the inner part. For mixed molecular ices (e.g., CO mixed with H₂O), the evaporation temperature depends on the type of mixed ice. Abundant but volatile species will rapidly sublimate as the mixed ice is heated up. However, a small abundance of these volatile species can remain trapped in the water ice in a clathrate-like structure. These minor species will not come off until the water ice itself starts to sublimate around 100 K. As evolution progresses, the envelope mass decreases and its overall temperature becomes higher.

Observational evidence for ice evaporation is found in both infrared and submillimeter data. Mid-IR spectra of CO and H₂O toward high-mass YSOs directly reveal changes in gas/solid ratios with increasing source temperature (van Dishoeck et al. 1996; Pontoppidan et al. 2003). Also, more complex molecules like HCN, C₂H₂, HNC and NH₃ freshly evaporated off the grains are found toward a few massive protostars, with orders of magnitude enhanced abundances compared with cold clouds (Evans et al. 1991; Lahuis & van Dishoeck 2000; Knez et al. 2008) (Fig. 5).

Independent evidence for freeze-out and evaporation comes from analysis of submillimeter data. The best fit to multi-transition CO data is obtained with a so-called ‘drop’ abundance profile (Fig. 2) in which the CO abundance is normal ($\sim 2 \times 10^{-4}$) in the warm inner part and in the outermost parts where the density is too low for significant freeze-out within the lifetime of the core. In the cold, dense intermediate zone, however, the abundance is at least an order of magnitude lower, since the timescale for freeze-out is short, $\sim 2 \times 10^9/n$ yr. This chemical structure, inferred from spatially unresolved data, has been confirmed by millimeter interferometer studies at higher angular resolution (~ 500 AU) for a selected set of objects where the freeze-out zone is directly imaged (e.g., Jørgensen 2004). It is also found for other molecules, especially those directly chemically related to CO.

4.3 Hot cores: complex organics and prebiotic molecules

In regions where the dust temperature reaches 90–100 K, even the most strongly-bound ices like H₂O start to evaporate, resulting in a ‘jump’ in the gas-phase abundances of molecules trapped in H₂O ice. For high-mass YSOs, this 100 K radius typically lies at 1000 AU, whereas for low-mass YSOs it is around 100 AU. Thus, taking typical source distances into account, these ‘hot cores’ have angular sizes of less than 1'' (Table 2), i.e., their emission is severely diluted in the $> 10''$ single-dish submillimeter beams. Other effects such as holes, cavities and disks also start to become important on these scales. Nevertheless, if the abundance enhancements are

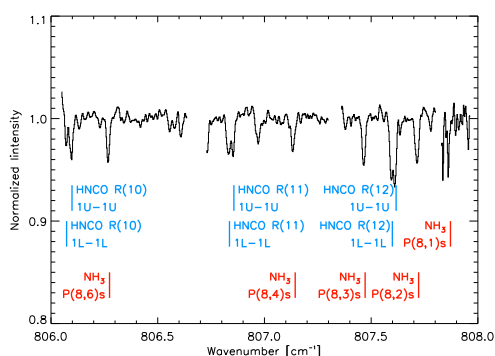


Fig. 5 Mid-IR spectrum toward the massive YSO NGC 7538 IRS1 showing high abundances of NH_3 and HNC in the hot core, likely freshly evaporated ices (Knez et al. 2008).

sufficiently large (typically more than a factor of 100), they can be detected even in unresolved data.

Hot core regions have been a prime focus of submillimeter observations for more than 30 years with line surveys focussing traditionally on the prototypical Orion and SgrB2 hot cores (e.g., Blake et al. 1987; Schilke et al. 2001; Nummelin et al. 2000) but now moving to more general high-mass regions (e.g., Helmich & van Dishoeck 1997; Gibb et al. 2000a) and even low-mass YSOs (e.g., Cazaux et al. 2003). Spectra of these objects are littered with lines and often confusion limited (Fig. 6). Indeed, such complex spectra are now used as signposts of sources in the earliest stages of massive star formation, since this stage even precedes the ultracompact H II region stage. Most of the lines can be ascribed to large, saturated organic molecules including CH_3OH (methanol), CH_3OCH_3 (di-methyl ether), HCOOCH_3 (methyl formate) and CH_3CN (methyl cyanide). With increasing frequency and sensitivity the laboratory line lists become more and more incomplete resulting in a large fraction of unidentified lines in observed data. For example, a recent 80–280 GHz IRAM-30m line survey of Orion-KL by Tercero & Cernicharo (in prep.) reveals 16000 lines of which 8000 were unidentified in 2005. Two years later, thanks to new laboratory data on just two molecules – $\text{CH}_3\text{CH}_2\text{CN}$ and CH_2CHCN – together with their isotopes and vibrationally excited states, the number of U-lines has been reduced to 6000. Significantly more laboratory work is needed to speed up this process. Also, the spectra of known molecules (including their isotopes and vibrationally excited states) need to be fully characterized and ‘weeded out’ before searches for new, more complex and pre-biotic species can be properly undertaken.

One of the main future questions is how far this chemical complexity goes. Molecules as complex as acetamide (CH_3CONH_2 , the largest interstellar molecule with a peptide bond) and glycol-aldehyde (CH_2OHCHO , the first interstellar ‘sugar’) have been found (e.g., Hollis et al. 2000; Hollis et al. 2006). However, in spite of literature claims, the simplest amino-acid glycine ($\text{NH}_2\text{CH}_2\text{COOH}$) has not yet

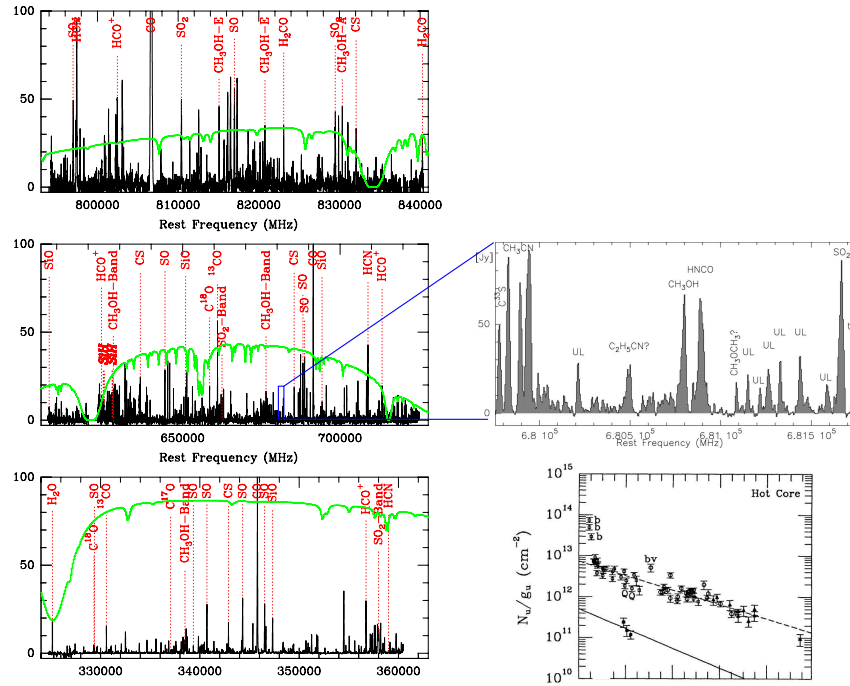


Fig. 6 Submillimeter line surveys of the Orion-KL region. Top: CSO 794-840 GHz survey by Comito et al. (2005); Middle: CSO 600-720 GHz survey by Schilke et al. (2001); Bottom: CSO 325-360 GHz line survey by Schilke et al. (1997). The green line in each panel indicates the typical atmospheric transmission. Right, middle: SMA interferometric survey around 680 GHz by Beuther et al. (2006). UL denotes unidentified lines. Right, bottom: rotation diagram of CH_3OH in the Orion hot core using JCMT data in the 345 GHz window by Sutton et al. (1995), giving $T_{\text{Tot}} \approx 250$ K (dashed line). The optically thin $^{13}\text{CH}_3\text{OH}$ lines give a somewhat lower temperature of ~ 180 K (full line).

been convincingly detected, although the chemically related amino acetonitrile ($\text{NH}_2\text{CH}_2\text{CN}$) has (Belloche et al. 2008). Other prebiotic species like aziridine and pyrimidine have also not yet been seen (Kuan et al. 2004). ALMA will be able to push the searches for larger, perhaps prebiotic molecules two orders of magnitude deeper to abundances of $< 10^{-13}$ with respect to H_2 , because it will have much higher sensitivity to compact emission and it will resolve the hot cores so that spatial information can be used to aid in the identification of lines. Indeed, chemical differentiation between, for example, O- and N-rich complex organics is seen on small spatial scales in both high- and low-mass YSOs from direct imaging (e.g., Wyrowski et al. 1999; Bottinelli et al. 2004) and is also inferred from (lack of) abundance correlations (Bisschop et al. 2007b, but see Fontani et al. 2007). Abundance ratios such as $\text{C}_2\text{H}_5\text{OH}/\text{CH}_3\text{OH}$ are remarkably constant in

high-mass YSOs, even in very diverse regions including the Galactic Center clouds (Requena-Torres et al. 2006), pointing toward a common origin for these O-rich organics. However, other O-containing molecules such as CH_2CO and CH_3CHO apparently avoid the warm gas, illustrating that not all complex organics co-exist (e.g., Ikeda et al. 2001; Bisschop et al. 2007b).

The origin of these complex organic molecules is still under debate, in particular whether they are first generation molecules directly evaporated from the ices or whether they are second generation products of a ‘hot core chemistry’ involving high-temperature gas-phase reactions between evaporated molecules (e.g., Charnley et al. 1992). A related problem is that the timescales for crossing the hot core region are very short for low-mass YSOs in a pure infall scenario, only a few hundred yr, much shorter than the timescales of $\sim 10^4 - 10^5$ yr needed for the hot core chemistry (Schöier et al. 2002). Thus, unless some mechanism has slowed down the infall or unless the molecules are in a dynamically stable region such as a disk, there is insufficient time for the hot core gas-phase chemistry to proceed.

4.4 Outflows and shocks

Bipolar outflows and jets are known to be associated with all embedded YSOs, both low- and high mass. They impact the quiescent envelope and create shocks which can sputter ices and, if sufficiently powerful, even the silicate grain cores themselves (e.g., Blake et al. 1995; Bachiller & Pérez-Gutiérrez 1997). The SiO molecule is therefore a good tracer of shocks: its abundance is greatly enhanced when Si atoms are liberated from the grains by the direct impact. Ices containing species like CH_3OH can be released in the less violent, turbulent shear zones. Indeed, in outflow lobes offset from the central protostar, CH_3OH is observed to be enhanced by more than two orders of magnitude (e.g., Jørgensen et al. 2004a; Benedettini et al. 2007). This could also provide an alternative explanation for the origin of the complex organic molecules, especially if most of them are formed on grains.

Owing to the high temperatures in shocks (up to a few 1000 K), reactions with energy barriers become very important in this hot gas compared with the colder cloud material. The most important example is the reaction of $\text{O} + \text{H}_2 \rightarrow \text{OH} + \text{H}$, followed by $\text{OH} + \text{H}_2 \rightarrow \text{H}_2\text{O} + \text{H}$ (reaction barriers ~ 2000 K), driving most of the atomic oxygen into water (e.g., Kaufman & Neufeld 1996). Thus, H_2O , OH and $[\text{O I}]$ far-infrared lines are predicted to dominate the shock emission, and this has been confirmed observationally for the Orion shock with ISO (Harwit et al. 1998). The precise balance between these three species depends on the H/H_2 ratio of the pre-shock gas, since reactions with H drive H_2O back to OH and O. Since lines of these species, together with those of CO and H_2 , are the main coolants of the gas, their observations also provide direct information on the energetics of the flows.

4.5 Water and the oxygen budget

Water is one of the most important molecules to study in protostellar and protoplanetary environments, because it is a dominant form of oxygen, the third most abundant element in the universe. Like CO, it thus controls the chemistry of many other species. Water also plays an important role in the energy balance as a strong gas coolant, allowing clouds to collapse up to higher temperatures. It can serve as a heating agent as well, if its levels are pumped by infrared radiation followed by collisional de-excitation. As discussed in §4.1, water is the most abundant molecule in icy mantles, and its presence may help the coagulation process that ultimately produces planets. Asteroids and comets containing ice have likely delivered most of the water to our oceans on Earth, where water is directly associated with the emergence of life. Thus, the distribution of water vapor and ice during the entire star and planet formation process is a fundamental problem relevant to our own origins.

Because water observations are limited from Earth, most information to date has come from satellites (see review by Cernicharo & Crovisier 2005). SWAS and ODIN observed the 557 GHz ground-state line of ortho-H₂O at poor spatial resolution, $\sim 3'$. The emission was found to be surprisingly weak, implying that most water is frozen out on grains in cold clouds, consistent with the direct ice observations. In contrast, ISO found hot water near massive protostars in mid-IR absorption line data (e.g., van Dishoeck et al. 1996; Boonman et al. 2003), as well as strong far-IR water emission lines near low-mass YSOs (e.g., Liseau et al. 1996; Ceccarelli et al. 1998; Nisini et al. 2002). The implication is that water undergoes orders of magnitude changes in abundance between cold and warm regions, from $\sim 10^{-8}$ up to 2×10^{-4} (Boonman & van Dishoeck 2003). Thus, water acts like a 'switch' that turns on whenever energy is deposited in molecular clouds, and it is a natural filter for warm gas.

An important question is the origin of the warm water seen near protostars. One option is shocks, as discussed in §4.4. ISO has detected strong H₂O and related OH and [O I] emission lines not only from Orion but also from low-mass YSO outflow lobes (e.g., Nisini et al. 1999). Another option is the quiescent inner warm envelope or hot core, where temperatures above ~ 230 K should be high enough to produce copious water both through ice evaporation and the above mentioned gas-phase reactions (Ceccarelli et al. 1996; Charnley 1997). Finally, an intriguing option is hot water arising from the accretion shock as material falls onto the disk. Indeed, strong mid-IR water lines have recently been detected with *Spitzer* with excitation conditions consistent with a disk accretion shock (Fig. 7, §5.1) (Watson et al. 2007).

A related puzzle is that of the total oxygen budget in clouds. Table 3 contains a summary of the various forms of oxygen for a cold dense cloud without star formation (Whittet et al. 2007; Pontoppidan et al. 2004). In low density diffuse clouds, optical and UV absorption line data have established that about 30% of the total (gas + solid) elemental O abundance of 4.6×10^{-4} is contained in refractory material such as silicates, with the remainder in gaseous atomic oxygen (Meyer et al. 1998). Assuming that the refractory budget stays the same in dense clouds, one can make an inventory of the remaining volatile components. As Table 3 shows, ices con-

Table 3 Typical oxygen budget in a quiescent cold cloud

Component	Material	Fraction of oxygen ^a	Observations
Refractory	Silicates	30%	Mid-IR, UV
Ices	H ₂ O, CO ₂ , CO, ...	26%	Mid-IR
Gas-phase	CO	9%	Submm, Mid-IR
Remainder	O? O ₂ ? H ₂ O?	35%	UV, Far-IR, Submm, Mid-IR

^a Values from Whittet et al. (2007) for several lines of sight in Taurus.

tain about 25–30% and gaseous CO up to 10% of the oxygen, with precise values varying from cloud to cloud. That leaves a significant fraction of the budget, about 1/3, unaccounted for. SWAS and ODIN have shown that the O₂ abundance in dense clouds is surprisingly low, $\leq 10^{-7}$ (Goldsmith et al. 2000; Larsson et al. 2007), as is H₂O in the cold gas (see above discussion). Thus, gaseous atomic O is the most likely reservoir. Limited data on [O I] 63 and 145 μ m emission or absorption from cold clouds exist (e.g., Caux et al. 1999; Vastel et al. 2002), but are difficult to interpret because of the high optical depth of the lines coupled with the fact that they are spectrally unresolved.

5 Protoplanetary disks

5.1 From envelope to disk

In §4, it has been shown that the inner envelopes around protostars contain a wealth of simple and complex molecules, but it is not yet clear whether and where these molecules end up in the planet-forming zones of disks since the dynamics of gas in the inner few hundred AU are poorly understood. In the standard theory for inside-out collapse and disk formation (e.g., Terebey et al. 1984; Cassen & Moosman 1981), most of the material enters the disk close to the centrifugal radius, which grows with time as t^3 . Also, the disk spreads as some material moves inward to accrete onto the star and some moves outward to conserve angular momentum. Thus, in the earliest phase of the collapse, gas falls in very close to the star where it will experience such a strong accretion shock that all ices evaporate and all molecules dissociate (Neufeld & Hollenbach 1994). However, at the later stages, once molecules enter the disks beyond a few AU, all species except the most volatile ices (e.g., CO ice) survive. Some observational evidence for accretion shocks has been presented through mid-IR CO observations (Pontoppidan et al. 2003) and H₂O data (Watson et al. 2007) (see Fig. 7).

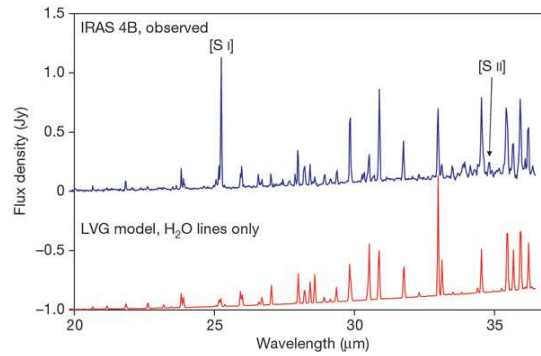


Fig. 7 Detection of hot water lines toward the deeply embedded Class 0 protostar NGC 1333 IRAS4B using the *Spitzer Space Telescope*. These lines are thought to originate from the accretion shock onto the growing disk (Watson et al. 2007).

5.2 Disk chemistry

Once in the disk, the chemistry of the outer part is governed by similar gas-phase and gas-grain interactions as in envelopes, but at higher densities. From analyses of SEDs, it is now well established that disks have temperature gradients not only in the radial direction but also vertically. If disks are flared, they intercept a large fraction of the stellar UV and X-rays which heat the dust and gas in the optically thin surface layers, with the IR emission from this layer subsequently warming the lower parts of the disk. Moreover, this radiation dissociates molecules and ionizes atoms, thus modifying the chemistry in the upper layers. The result is a layered chemical structure (Aikawa et al. 2002), with a cold mid-plane where most molecules are frozen out, a top layer consisting mostly of atoms, and an intermediate layer where the dust grains are warm enough to prevent complete freeze-out and where molecules are sufficiently shielded from radiation to survive (for review, see Bergin et al. 2007).

5.2.1 Outer disk

Indirect evidence for freeze-out in disks comes from the inferred low gas-phase abundances of various molecules (e.g., Dutrey et al. 1997; van Zadelhoff et al. 2001). Direct detection of ices in disks has been possible for a few sources with a favorable near edge-on geometry where the line of sight passes through the outer part (e.g., Pontoppidan et al. 2005; Terada et al. 2007). Because foreground clouds can also contribute to the observed ice absorptions, it has not yet been possible to make an ice inventory for disks. At longer wavelengths, the ice bands can be emission, and therefore do not require a special geometry. Bands of crystalline water ice at 45 and 62 μm have been seen in a few disks with ISO (e.g., Creech et al. 2002).

Most molecules other than CO have only been detected in spatially unresolved single-dish submillimeter spectra from which disk-averaged abundances can be derived (e.g., Dutrey et al. 1997; Thi et al. 2004). Chemical ‘images’ of disks have so far been limited to just a few pixels across a handful of disks in a few lines (e.g., Qi et al. 2003; Dutrey et al. 2007). The data obtained so far support the layered structure picture but obviously ALMA will throw this field wide open. Besides being interesting in its own right, chemistry and molecular lines can also constrain important physical processes in disks, such as the level of turbulence and the amount of vertical mixing (e.g., Semenov et al. 2006).

5.2.2 Inner disk

The hot gas in the inner disk is readily detected in the mid-IR lines of CO (e.g., Najita et al. 2003; Blake & Boogert 2004), as well as the UV and IR lines of H₂ (e.g., Herczeg et al. 2002; Martin-Zaïdi et al. 2007). PAH emission has also been spatially resolved, with both the inner and outer disk contributing to the various features (e.g., Habart et al. 2004; Geers et al. 2007). The chemistry in the inner disk differs in several aspects from that in the outer parts: the densities are so high that three-body reactions become important; X-rays from the young star may be significant; gas columns may be so high that cosmic rays can no longer penetrate to the mid-plane, thus stopping ion-molecule reactions; and Fischer-Tropsch catalysis can take place on hot metallic grains. A particularly exciting topic is the chemistry inside the ‘snow-line’ where all molecules evaporate and the chemistry approaches that at LTE (e.g., Markwick et al. 2002). *Spitzer* absorption line data have revealed highly abundant and hot (300–700 K) HCN and C₂H₂ in the inner few AU of two young near edge-on disks consistent with these models (Lahuis et al. 2006; Gibb et al. 2007). More recently, *Spitzer* and ground-based Keck and VLT data have revealed surprisingly strong mid-IR emission lines of hot H₂O (~800 K), together with OH, HCN, C₂H₂ and/or CO₂, toward a number of disks originating from the inner AU (Carr & Najita 2008; Salyk et al. 2008).

5.3 Disk chemical evolution

Near- and mid-infrared surveys have shown that inner dust disks (<10 AU) disappear on timescales of a few Myr (e.g., Cieza et al. 2007). A major question is how the gas and dust dissipate from the disk, and whether they do so at the same time. Examination of hundreds of SEDs of stars with disks in *Spitzer* surveys show that there may be multiple evolutionary paths from the massive gas-rich disks to the tenuous gas-poor debris disks, involving both grain growth and gap opening, either by photoevaporation or planet formation (e.g., Alexander et al. 2006; Varnière et al. 2006). Some transitional disks show evidence that molecular gas and PAHs are still present inside the dust gaps (Goto et al. 2006; Jonkheid et al. 2006;

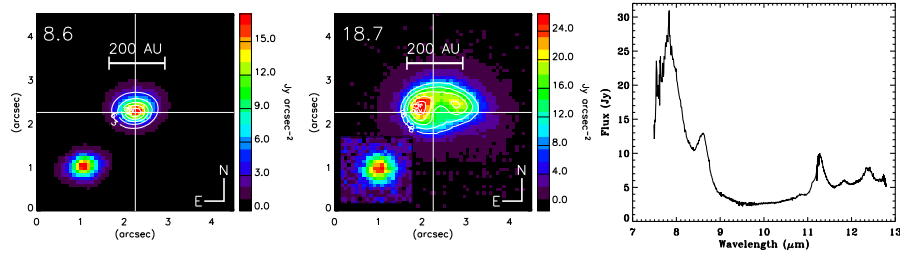


Fig. 8 VLT-VISIR mid-infrared images of the disk around the young T Tauri star IRS 48, showing strong centrally peaked PAH emission at $11.3 \mu\text{m}$ as well as a 60 AU diameter gap devoid of large grains emitting at $19 \mu\text{m}$. The inserts show the PSF of a standard star. The 8–13 μm spectrum with the strong PAH features is included (Geers et al. 2007).

Geers et al. 2007; Pontoppidan et al. 2008) (see Fig. 8). [O I] is the dominant coolant of dense gas, and as such may also be a particularly powerful gas mass probe of transitional disks with future facilities (Meijerink et al. 2008). The chemistry with such high gas/dust ratios and large grains (which inhibit H_2 formation) is very different from that under normal cloud conditions (e.g., Aikawa & Nomura 2006; Jonkheid et al. 2007). Moreover, the shape of the radiation field plays a critical role, in particular whether there are far-UV photons with energies $>11 \text{ eV}$ which can dissociate H_2 and CO and ionize C (van Zadelhoff et al. 2003; van Dishoeck et al. 2006). Also, young stars are known to have UV flares resulting from discrete accretion events, which temporarily increase the disk temperature and affect the chemistry.

6 Prospects for future facilities

The major new facilities at infrared and submillimeter wavelengths will be crucial to answer many of the questions raised in the previous sections. The principle limitation at millimeter wavelengths is the low spatial resolution and sensitivity: current single-dish telescopes and interferometers can hardly resolve the envelopes, hot cores and disks. ALMA will be a tremendous leap forward in this field, with the capability and sensitivity to image molecules down to scales of tens of AU where planet formation takes place. In the coldest pre-stellar cores, ALMA can detect the earliest signs of collapse through line profiles of species like N_2H^+ and ortho- H_2D^+ on 100 AU scales. Once the protostar has formed, ALMA is the instrument of choice to unravel the chemistry in hot cores and search for the most complex prebiotic molecules, by spatially imaging the organics and ‘weeding out’ the more common species. Low-frequency cm data, such as could be provided by one version of the proposed Square Kilometer Array, are well suited to probe the heaviest rotors. ALMA can also resolve individual bowshocks and thus distinguish the shock chemistry from that of the other protostellar components. For example,

are the complex organics located in the passively heated hot core region, in the disk, or in the region where the outflow impacts the dense envelope?

Studies of the chemistry in outer disk will be opened up completely by ALMA, which will provide chemical images in many different species. Since the brightness temperatures of the submillimeter lines from the inner disk can be as high as several hundred K, ALMA can image lines in the nearest disks down to ~ 10 AU. Because of lower optical depth, ALMA has the advantage that it can probe deeper into the disk than infrared telescopes. ALMA will also be critical to study transitional objects by imaging the holes or gaps in their dust disks down to a few AU and by measuring the remaining gas mass through tracers like CO and [C I] on scales of more than 10 AU.

The strength of JWST-MIRI and NIRSPEC lies in their raw sensitivity coupled with moderate spectral resolution. They will be particularly powerful to probe the ices in the densest, most obscured parts of the cores and determine when and where ices are formed through ice mapping on $\sim 10''$ scale. The high sensitivity will also allow searches for minor ice species toward highly obscured Class 0 protostars to address the question, together with ALMA, which (complex) molecules are formed on the grains as first generation species and which in the gas as second generation. Mid-IR imaging of shocked H_2 , [S I] and [Fe II] with JWST will trace the physical structure of shocks in the deeply embedded phase, necessary for understanding the chemistry.

JWST will also allow observations of ices toward a much larger fraction of edge-on disks, and can perhaps even spatially resolve the absorption against the extended mid-IR continuum. Moreover, with its medium resolution mode $R \approx 3000$, JWST can search for mid-infrared vibration-rotation lines of water and organic building blocks like HCN, C_2H_2 and CH_4 in absorption or emission in protostars and disks, although analysis will be hampered by the fact that the lines are spectrally unresolved.

The unique power of ground-based ELTs lies in their very high spectral resolving power up to 10^5 combined with high sensitivity and spatial resolution, allowing quantitative studies of gas-phase lines. Toward protostellar objects, gas/dust ratios can be measured directly in the coldest regions, and some of the complex organics freshly evaporated off the grains can be probed in absorption even toward solar-mass sources. Emission lines of hot water and organics from disks should have booming feature-to-continuum ratios and such spectra will also allow searches for less common species. Moreover, ELTs can image the emission and kinematics at AU resolution and thus determine the chemistry *distribution* in the inner (< 10 AU) disk, which ALMA cannot probe. This includes the distribution of PAHs, the most complex organics known to date.

Herschel's strength lies in its ability to observe cold and warm H_2O in protostellar environments through the myriad of pure rotational lines. Indeed, the combination of Herschel and SOFIA will be uniquely suited to observe H_2O , OH and O far-infrared lines with orders of magnitude higher spatial and/or spectral resolution and sensitivity compared with previous missions. With no other far-infrared space missions on the horizon, this will be the only chance for decades to follow the water

trail through star formation and determine the oxygen budget in a variety of sources. SOFIA is a key complement to Herschel, since it is the only mission that can provide spectrally resolved data on the [O I] lines at 63 and 145 μm .

Herschel and SOFIA will also fully open up the far-infrared wavelength range through line surveys, with ample opportunities for unexpected chemical surprises. Higher frequency THz data can help in the identification of more complex species (including PAHs) since their low-frequency vibrational modes may be more easily recognized than their pure rotational spectra observed with ALMA, where the intensity is spread over many lines. SOFIA will also be the only instrument available to probe the lowest 1370 GHz transition of para- H_2D^+ in the coldest clouds whereas both SOFIA and Herschel can observe the lowest ortho- D_2H^+ transition at 1476 GHz. Finally, Herschel and SOFIA can search for the far-infrared bands of ices and (hydrated) silicates in emission from protostars and disks. This is the only option to probe ices in disks which do not require any special viewing geometry.

7 Conclusions

Substantial progress has been made in determining the inventories of the gases and solids in protostellar and protoplanetary regions, not only for bright high-mass YSOs but also for weaker sources thought to be representative of our own early solar system. Each evolutionary phase has its own chemical characteristics related to the changing physical conditions, with freeze-out and ice evaporation playing a major role. The combination of observations from near-infrared to millimeter wavelengths has been essential to probe all chemical components. Basic laboratory data and sophisticated radiative transfer tools remain crucial for quantitative analysis. With the orders of magnitude enhancements in sensitivity, spatial and spectral resolution of future instruments, there is no doubt that astrochemistry will continue to blossom in the next decade of JWST and its concurrent facilities.

Acknowledgements I am grateful to the editor A.G.G.M. Tielens for comments, and to moderator of this session, J. Cernicharo, for stimulating the discussion, the content of which has been included in this chapter. This work is supported by a Spinoza grant from the Netherlands Organization for Scientific Research (NWO).

References

- Aikawa, Y., & Nomura, H. 2006, *ApJ*, 642, 1152
Aikawa, Y., van Zadelhoff, G.J., van Dishoeck, E.F., & Herbst, E.F. 2002, *A&A*, 386, 622
Alexander, R.D., Clarke, C.J., & Pringle, J.E. 2006, *MNRAS*, 369, 229
Bachiller, R., Pérez-Gutiérrez, M. 1997, *ApJ*, 487, L93

- Belloche, A., Menten, K.M., Comito, C., Mueller, H.S.P., Schilke, P., Ott, J., Thorwirth, S., & Hieret, C. 2008, *A&A*, in press
- Benedettini, M., Viti, S., Codella, C., et al. 2007, *MNRAS*, 381, 1127
- Bergin, E. A., Aikawa, Y., Blake, G. A., & van Dishoeck, E. F. 2007, in *Protostars and Planets V*, ed. B. Reipurth, D. Jewitt, & K. Keil, 751–766
- Bergin, E.A., Tafalla, M. 2007, *ARA&A* 45, 339
- Bergin, E. A., Alves, J., Huard, T., & Lada, C. J. 2002, *ApJ*, 570, L101
- Bergin, E.A., Melnick, G.J., Stauffer, J.R., et al. 2000, *ApJ*, 539, L129
- Beuther, H., Zhang, Q., Reid, M.J., et al. 2006, *ApJ*, 636, 323
- Bisschop, S. E., Fuchs, G.W., van Dishoeck, E. F., & Linnartz, H. 2007a, *A&A*, 474, 1061
- Bisschop, S. E., Jørgensen, J. K., van Dishoeck, E. F., & de Wachter, E. B. M. 2007b, *A&A*, 465, 913
- Bisschop, S.E., Jørgensen, J.K., Bourke, T., Bottinelli, S., & van Dishoeck, E.F. 2008, *A&A*, submitted
- Blake, G.A., & Boogert, A.C.A. 2004, *ApJ*, 606, L73
- Blake, G.A., Sutton, E.C., Masson, C.R., & Phillips, T.G. 1987, *ApJ*, 315, 621
- Blake, G.A., Sandell, G., van Dishoeck, E.F., Aspin, C., Groesbeck, T., & Mundy, L.G. 1995, *ApJ*, 441, 689
- Boogert, A., Pontoppidan, K., Knez, C., et al. 2008, *ApJ*, in press
- Boogert, A., Pontoppidan, K., Lahuis, F., et al. 2004, *ApJS*, 154, 359
- Boonman, A.M.S., Doty, S.D., van Dishoeck, E.F., Bergin, E.A., Melnick, G.J., Wright, C.M., & Stark, R. 2003, *A&A*, 406, 937
- Boonman, A.M.S. & van Dishoeck, E.F. 2003, *A&A*, 403, 1003
- Bottinelli, S., Ceccarelli, C., Williams, J. P., & Lefloch, B. 2007, *A&A*, 463, 601
- Bottinelli, S., Ceccarelli, C., Neri, R., et al. 2004, *ApJ*, 617, L69
- Brünken, S., Gupta, H., Gottlieb, C.A., McCarthy, M.C., & Thaddeus, P. 2007, *ApJ*, 664, L43
- Butner, H.M., Charnley, S.B., Ceccarelli, C., et al. 2007, *ApJ*, 659, L137
- Carr, J.S., & Najita, J. 2008, *Science*, 319, 1504
- Caselli, P., Walmsley, C. M., Tafalla, M., Dore, L., & Myers, P. C. 1999, *ApJ*, 523, L165
- Caselli, P., van der Tak, F.F.S., Ceccarelli, C., & Bacmann, A. 2003, *A&A*, 403, L37
- Cassen, P., & Moosman, A. 1981, *Icarus*, 48, 353
- Caux, E., Ceccarelli, C., Castets, A., Vastel, C., Liseau, R., Molinari, S., Nisini, B., Saraceno, P., & White, G.J. 1999, *A&A*, 347, L1
- Cazaux, S., Tielens, A.G.G.M., Ceccarelli, C., et al. 2003, *ApJ*, 593, L51
- Ceccarelli, C., Hollenbach, D.J., & Tielens, A.G.G.M. 1996, *ApJ*, 471, 400
- Ceccarelli, C., Caux, E., White, G.J., et al. 1998, *A&A*, 331, 372
- Ceccarelli, C., Caselli, P., Herbst, E., Tielens, A. G. G. M., & Caux, E. 2007, in *Protostars and Planets V*, ed. B. Reipurth et al., 47–62
- Cernicharo, J., Crovisier, J. 2005, *Space Science Rev.*, 119, 29
- Chandler, C.J., Brogan, C.L., Shirley, Y.L., & Loinard, L. 2005, *ApJ*, 632, 371
- Charnley, S.B. 1997, *ApJ*, 481, 396
- Charnley, S.B., Tielens, A.G.G.M., & Millar, T.J. 1992, *ApJ*, 399, L71

- Cieza, L., Padgett, D.L., Stapelfeldt, K.R., et al. 2007, *ApJ*, 667, 308
- Comito, C., Schilke, P., Phillips, T.G., Lis, D.C., Motte, F., & Mehringer, D. 2005, *ApJS*, 156, 127
- Creech-Eakman, M.J., Chiang, E.I., Joungh, R.M.K., Blake, G.A., & van Dishoeck, E.F. 2002, *A&A*, 385, 546
- Dutrey, A., Guilloteau, S., Duvert, G., Prato, L., Simon, M., Schuster, K., Menard, F. 1996, *A&A*, 309, 493
- Dutrey, A., Guilloteau, S., Guelin, M. 1997, *A&A*, 317, L55
- Dutrey, A., Henning, Th., Guilloteau, S., et al. 2007, *A&A*, 464, 615
- Evans, N.J., Lacy, J.H., Carr, J.S. 1991, *ApJ*, 383, 674
- Fontani, F., Pascucci, I., Caselli, P., Wyrowski, F., Cesaroni, R., & Walmsley, C.M. 2007, *A&A*, 470, 639
- Garrod, R.T., Herbst, E. 2006, *A&A*, 457, 927
- Gerakines, P.A., Schutte, W.A., & Ehrenfreund, P. 1996, *A&A*, 312, 289
- Geers, V.C., Augereau, J.-C., Pontoppidan, K.M., et al. 2006, *A&A*, 459, 545
- Geers, V.C., Pontoppidan, K.M., van Dishoeck, E.F., et al. 2007, *A&A*, 469, L35
- Gibb, E.L., Nummelin, A., Irvine, W.M., Whittet, D.C.B., Bergman, P. 2000a, *ApJ*, 545, 309
- Gibb, E.L., Whittet, D.C.B., Schutte, W.A. et al. 2000b, *ApJ*, 536, 346
- Gibb, E.L., van Brunt, K.A., Brittain, S.D., & Rettig, T.W. 2007, *ApJ*, 660, 1572
- Goldsmith, P.F., Melnick, G.J., Bergin, E.A., et al. 2000, *ApJ*, 539, L123
- Goto, M., Stecklum, B., Linz, H., Feldt, M., Henning, Th., Pascucci, I., & Usuda, T. 2006, *ApJ*, 649, 299
- Habart, E., Natta, A., Krügel, E. 2004, *A&A*, 427, 179
- Harwit, M., Neufeld, D.A., Melnick, G.J., & Kaufman, M.J. 1998, *ApJ*, 497, L105
- Helmich, F.P., van Dishoeck, E.F. 1997, *A&AS*, 124, 205
- Herczeg, G.J., Linsky, J.L., Valenti, J.A., Johns-Krull, C.M., & Wood, B.E. 2002, *ApJ*, 572, 310
- Hollis, J. M., Lovas, F. J., & Jewell, P. R. 2000, *ApJ*, 540, L107
- Hollis, J. M., Lovas, F. J., Remijan, A. J., et al. 2006, *ApJ*, 643, L25
- Hudgins, D.M., Sandford, S.A., Allamandola, L.J., & Tielens, A.G.G.M. 1993, *ApJS*, 86, 713
- Hudgins, D.M., Allamandola, L.J. 1999, *ApJ*, 516, L41
- Ikedo, M., Ohishi, M., Nummelin, A., Dickens, J.E., Bergman, P., Hjalmarsen, Å, & Irvine, W.M. 2001, *ApJ*, 560, 792
- Kaufman, M.J., & Neufeld, D.A. 1996, *ApJ*, 456, 611
- Lada, C.J. 1999, in *The Origin of Stars and Planetary Systems*, ed. C.J. Lada & N.D. Kylafis (Dordrecht: Kluwer), p. 143
- Lahuis, F., & van Dishoeck, E.F. 2000, *A&A*, 355, 699
- Larsson, B., Liseau, R., Pagani, L., et al. 2007, *A&A*, 466, 999
- Jaeger, C., Molster, F.J., Dorschner, J., Henning, Th., Mutschke, H., Waters, L.B.F.M. 1998, *A&A*, 339, 904
- Jonkheid, B., Kamp, I., Augereau, J.-C., & van Dishoeck, E.F. 2006, *A&A*, 453, 163

- Jonkheid, B., Dullemond, C.P., Hogerheijde, M.R., & van Dishoeck, E.F. 2007, *A&A*, 463, 203
- Jørgensen, J.K. 2004, *A&A*424, 589
- Jørgensen, J. K., Bourke, T. L., Myers, P. C., et al. 2007, *ApJ*, 659, 479
- Jørgensen, J. K., Bourke, T. L., Myers, P. C., et al. 2005, *ApJ*, 632, 973
- Jørgensen, J.K., Hogerheijde, M.R., Blake, G.A., van Dishoeck, E.F., Mundy, L.G., & Schöier, F.L. 2004, *A&A*, 415, 1021
- Jørgensen, J.K., Schöier, F.L., & van Dishoeck, E.F. 2004, *A&A*, 416, 603
- Keane, J.V., Tielens, A.G.G.M., Boogert, A.C.A., Schutte, W.A., & Whittet, D.C.B. 2001, *A&A*, 376, 254
- Knez, C., Lacy, J., Evans, N.J., II, et al. 2008, *ApJ*, in press
- Kuan, Y-J., Charnley, S.B., Huang, H-C., Kisiel, Z., Ehrenfreund, P., Tseng, W-L., & Yan, C-H. 2004, *Adv. Space Res.*, 33, 31
- Lahuis, F., van Dishoeck, E. F., Boogert, A. C. A., et al. 2006, *ApJ*, 636, L145
- Lis, D.C, Roueff, E., Gerin, M., Phillips, T.G., Coudert, L.H., van der Tak, F.F.S., & Schilke, P. 2002, *ApJ* 571, L55
- Liseau, R., Ceccarelli, C., Larsson, B., et al. 1996, *A&A*, 315, L181
- Marcelino, N., Cernicharo, J., Agúndez, M., et al. 2007, *ApJ*, 665, L127
- Markwick, A.J., Ilgner, M., Millar, T.J., & Henning, Th. 2002, *A&A*, 385, 632
- Martin-Zaïdi, C., Lagage, P-O., Pantin, E., & Habart, E. 2007, *ApJ*, 666, L117
- McCarthy, M.C., Gottlieb, C.A., Gupta, H., & Thaddeus, P. 2006, *ApJ*, 652, L141
- Meijerink, R., Glassgold, A.E., & Najita, J.R. 2008, *ApJ*, in press
- Meyer, D.M., Jura, M., & Cardelli, J.A. 1998, *ApJ*, 493, 222
- Najita, J., Carr, J.S., & Mathieu, R.D. 2003, *ApJ*, 589, 931
- Neufeld, D. A. & Hollenbach, D. J. 1994, *ApJ*, 428, 170
- Nisini, B., Benedettini, M., Giannini, T., et al. 1999, *A&A*, 350, 529
- Nisini, B., Giannini, T., Lorenzetti, D. 2002, *ApJ*, 574, 246
- Noriega-Crespo, A., Morris, P., Marleau, F.R., et al. 2004, *ApJS*, 154, 352
- Nummelin, A., Bergman, P., Hjalmarsen, Å, et al. 2000, *ApJS*, 128, 213
- Öberg, K.I., van Broekhuizen, F., Fraser, H.J., Bisschop, S.E., van Dishoeck, E.F., & Schlemmer, S. 2005, *ApJ*, 621, L33
- Öberg, K.I., Fraser, H.J., Boogert, A.C.A., Bisschop, S.E., Fuchs, G.W., van Dishoeck, E.F., & Linnartz, H. 2007, *A&A*, 462, 1187
- Parise, B., Castets, A., Herbst, E., Caux, E., Ceccarelli, C., Mukhopadhyay, I., & Tielens, A.G.G.M. 2004, *A&A*, 416, 159
- Pillai, T., Wyrowski, F., Hatchell, J., Gibb, A.G., & Thompson, M.A. 2007, *A&A*, 467, 207
- Pontoppidan, K.M., Blake, G.A., van Dishoeck, E.F., Smette, A., Ireland, M.I., & Brown, J.M. 2008, *ApJ*, in press
- Pontoppidan, K.M., Fraser, H.J., Dartois, E., et al. 2003, *A&A*, 408, 981
- Pontoppidan, K.M., van Dishoeck, E.F., & Dartois, E. 2004, *A&A*, 426, 925
- Pontoppidan, K.M., Dullemond, C.P., van Dishoeck, E.F., et al. 2006, *ApJ*, 622, 463
- Pontoppidan, K.M. 2006, *A&A*, 453, L47
- Qi, C., Kessler, J. E., Koerner, D. W., Sargent, A. I., & Blake, G. A. 2003, *ApJ*, 597, 986

- Requena-Torres, M.A., Martín-Pintado, J., Rodríguez-Franco, A., Martín, S., Rodríguez-Fernández, N.J., & de Vicente, P. 2006, *A&A*, 455, 971
- Roberts, H., Herbst, E., & Millar, T.J. 2003, *ApJ*, 591, L41
- Salyk, C., Pontoppidan, K.M., Blake, G.A., Lahuis, F., van Dishoeck, E.F., & Evans, N.J. 2008, *ApJ*, 676, L49
- Schilke, P., Benford, D.J., Hunter, T.R., Lis, D.C., & Phillips, T.G. 2001, *ApJS*, 132, 281
- Schilke, P., Groesbeck, T.D., Blake, G.A., & Phillips, T.G. 1997, *ApJS*, 108, 301
- Schöier, F.L., Jørgensen, J.K., van Dishoeck, E.F., & Blake, G.A. 2002, *A&A*, 390, 1001
- Schöier, F.L., van der Tak, F.F.S., van Dishoeck, E.F., & Black, J.H. 2005, *A&A*, 432, 369
- Schutte, W.A., Khanna, R.K. 2003, *A&A*, 398, 1049
- Semenov, D., Wiebe, D., & Henning, Th. 2006, *ApJ*, 647, L57
- Snell, R.L., Howe, J.E., Ashby, M.L.N., et al. 2000, *ApJ*, 539, L101
- Sutton, E.C., Peng, R., Danchi, W.C., Jaminet, P.A., Sandell, G., Russell, A.P.G. 1995, *ApJS*, 97, 455
- Terada, H., Tokunaga, A.T., Kobayashi, N., Takato, N., Hayano, Y., & Takami, H. 2007, *ApJ*, 667, 303
- Terebey, S., Shu, F.H., & Cassen, P. 1984, *ApJ*, 286, 529
- Thi, W.-F., van Zadelhoff, G.-J., & van Dishoeck, E.F. 2004, *A&A*, 425, 955
- Thi, W.-F., & Bik, A. 2005, *A&A*, 438, 557
- Tielens, A.G.G.M. 1983, *A&A*, 119, 177
- Tielens, A.G.G.M. 2008, *ARA&A*, in press
- Tielens, A.G.G.M., Charnley, S.B. 1997, *Origins Life Evol. B.*, 27, 23
- Tielens, A.G.G.M., Hagen, W. 1982, *A&A*, 114, 245
- van Broekhuizen, F.A., Pontoppidan, K.M., Fraser, H.J., & van Dishoeck, E.F. 2005, *A&A*, 441, 249
- van der Tak, F. F. S., Caselli, P., & Ceccarelli, C. 2005, *A&A*, 439, 195
- van Dishoeck, E. F. 2004, *ARA&A*, 42, 119
- van Dishoeck, E. F. 2006, *Proc. Nat. Ac. Science*, 103, 12249
- van Dishoeck, E.F. & Blake, G.A. 1998, *ARA&A*, 36, 317
- van Dishoeck, E. F., van Hemert, M.C., & Jonkheid, B.J. 2006, *Faraday Discussions*, 133, 231
- van Dishoeck, E.F., Helmich, F.P., de Graauw, T., et al. 1996, *A&A*, 315, L349
- van Zadelhoff, G.-J., van Dishoeck, E.F., Thi, W.-F., & Blake, G.A. 2001, *A&A*, 377, 566
- van Zadelhoff, G.-J., Dullemond, C.P., van der Tak, F.F.S., et al. 2002, *A&A* 395, 373
- van Zadelhoff, G.-J., Aikawa, Y., Hogerheijde, M.R., & van Dishoeck, E.F. 2003, *A&A*, 397, 789
- Varnière, P., Blackman, E.G., Frank, A., & Quillen, A.C. 2006, *ApJ*, 640, 1110
- Vastel, C., Phillips, T.G., & Yoshida, H. 2004, *ApJ*, 606, L127
- Vastel, C., Polehampton, E.T., Baluteau, J.-P., Swinyard, B.M., Caux, E., & Cox, P. 2002, *ApJ*, 581, 315

- Wakelam, V., Herbst, E., & Selsis, F. 2006, *A&A*, 451, 551
- Watanabe, N., Nagaoka, A., Shiraki, T., & Kouchi, A. 2004, *ApJ*, 616, 638
- Watson, D.M., Bohac, C.J., Hull, C., et al. 2007, *Nature*, 448, 1026
- Whittet, D.C.B., Shenoy, S.S., Bergin, E.A., et al. 2007, *ApJ*, 655, 332
- Wyrowski, F., Schilke, P., Walmsley, C.M., & Menten, K.M. 1999, *ApJ*, 514, L43
- Young, C.H., Jørgensen, J.K., Shirley, Y.L., et al. 2004, *ApJS*, 154, 352